Int. J. Multiphase Flow Vol. 12, No. 4, pp. 575–585, 1986
Printed in Great Britain

0301-9322/86 $3.00 + .00
Pergamon Journals/Elsevier

TWO-PHASE FLOW IN A *T*-JUNCTION WITH A HORIZONTAL INLET

PART I: PHASE SEPARATION

W. SEEGER, J. REIMANN and U. MÜLLER
Kernforschungszentrum Karlsruhe, Institut für Reaktorbauelemente, Postfach 3640,
7500 Karlsruhe 1, Federal Republic of Germany

(*Received* 31 *May* 1985; *in revised form* 10 *October* 1985)

Abstract—Phase separation was measured in air–water and steam–water mixtures flowing through a *T*-junction with equal pipe diameters (d = 50 mm) and a horizontal, vertical upward or vertical downward branch. The flow parameters were varied over a wide range to generate a variety of inlet flow patterns. The degree of phase separation depends significantly on the branch orientation, the inlet flow pattern and the ratio of inlet mass flux to branch mass flux. Empirical correlations for the phase separation for the different branch orientations have been derived.

1. INTRODUCTION

When a two-phase mixture is divided in a *T*-junction, the branch and run qualities x_3 and x_2 in general differ from the inlet quality x_1. This phase separation is influenced by three effects:

(1) The different inertia of the phases: in general, the lighter phase preferentially enters the branch.
(2) The flow pattern in the inlet: the influence of the phase and velocity distribution in the inlet cross section depends on the branch angle with respect to the horizontal inlet and the branch to inlet diameter ratio d_3/d_1. For a horizontal inlet, the flow patterns are dominated by gravity for a wide range of flow parameters.
(3) Gravity effects in the branch: for inclined branches flow reversal of one phase can occur.

Until now there exists no general method to predict this flow behavior for arbitrary flow conditions and *T*-junction geometries. Due to the large number of parameters, the experimental data base is also very limited.

Experimental results, closely related to the present ones, were presented by Saba & Lahey (1982, 1984) for air–water flow through a horizontal *T*-junction (all pipes in the horizontal plane). The flow parameters were subjected to much less variation than in the present experiments. These authors were the first to present a closed physical-based empirical model which included the phase separation and pressure differences in the *T*-junction.

Other contributions related to the present investigations are due to Henry (1981), Honan & Lahey (1981), Azzopardi & Baker (1981), Azzopardi & Whalley (1982), Zetzmann (1982) and Smoglie & Reimann (1986).

This article summarizes experimental investigations with *T*-junctions of equal diameters (d = 50 mm), a horizontal inlet flow, and a horizontal, vertical upward or downward orientation of the branch. The experiments were performed with air–water flow (maximum pressure p_1 < 1 MPa), steam–water flow (p_{max} < 10 MPa) and an inlet mass flux range $500 < G_1 < 7000$ kg/m^{2}s including different flow patterns; the ratio of the branch mass flux G_3 to the inlet mass flux G_1 was varied between 0 and 1. Detailed results and all data were published by Seeger (1985); additional aspects on the phase separation phenomena were discussed by Seeger *et al.* (1985).

Part I of this article presents results on the phase separation phenomena. In part II, results on the pressure differences in the *T*-junction are reported.

2. TEST LOOP AND TEST PROCEDURE

The test facility, described in detail by John & Reimann (1979), enables air–water experiments with maximum flow rates of 30 kg/s for water and about 1 kg/s for air; the maximum pressure is about 1 MPa. The maximum capacity of the steam–water loop is about 5 kg/s. The quality can be varied between 0 and 1. The maximum pressure is 15 MPa. The mass flow rates are measured separately under single-phase conditions, and these flows are then mixed in a mixing chamber.

The test section consisted of the horizontal inlet pipe (length about 2 m) between the mixing chamber and the T-junction, followed by the horizontal run of 3 m length. The branch pipe was installed either horizontally, vertically upward or downward; the corresponding lengths were 3.1, 2.1, or 0.76 m. All pipes of the test section had inner diameters of 50 mm and were made from carbon steel. For flow visualization studies, the T-junction and some pipes were made from plexiglas.

Figure 1 shows that particular part of the test facility which was specially built for the present experiments: the flow is divided in the T-junction by means of the branch valve and the run valve. The branch valve is operated by hand, the run valve is an automatic control valve which keeps the pressure in the test section at a given value. The mixtures are throttled in the valves to a maximum pressure of 0.5 MPa and flow to specially designed separators. The water exits from the bottom, and the air or steam from the top of these vessels. Due to the wide range of mass flow rates ($0.024 < \dot{m}_L < 30$ kg/s, $0.001 < m_G < 3$ kg/s) three measurement sections are installed for the gas phase and four for the liquid phase. These sections are equipped with variable throttle meters (Durchfluβmeβgerät CD, Fa. Caldyn, Ettlingen, FRG), which are calibrated for two different throttle positions. For steam–water experiments the measurement sections can be cooled or heated to guarantee single-phase conditions.

Further downstream, the single-phase flow again enters a mixing chamber followed by an automatic control valve to keep the pressure in the separator system at a given value. The mixtures of the run and branch finally join and flow to the steam condenser or air–water separator.

The optimum operating behavior of the run and branch separators is of great importance. On the one hand, the gas–liquid interface (and with this the vessel diameter) has to be large at large volume flow rates to prevent gas or liquid entrainment. On the other hand, measurement errors occur if the height of the interface in the separator is not constant. For a large vessel diameter, very small changes of the interface level cause considerable errors in case of low volume flow rates. Therefore, the separators used have different cross sections and a height of more than 7 m, as shown in figure 2. Depending on the flow rates, the interface was set to a level where entrainment did not occur but good level control was possible.

The complexity of the system, required exceptionally high service to perform the experiments. For selected flow conditions in the inlet (pressure p_1, mass flux G_1, quality x_1) the mass flux ratio G_3/G_1 was varied between zero (closed branch valve) and unity (closed run valve). Up to ten split points were established. For each split point appropriate measurement sections had to be chosen and the interface levels (measured by differential pressure transducers) had to be selected and controlled. When the total system was stabilized,

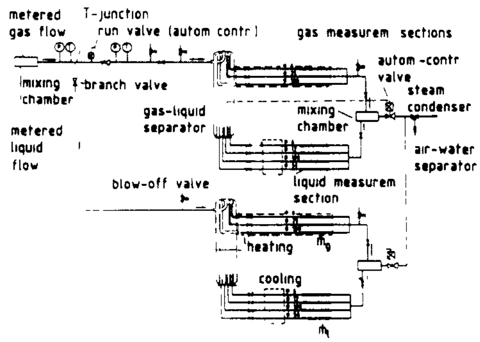

Figure 1 Test section and measurement set-up

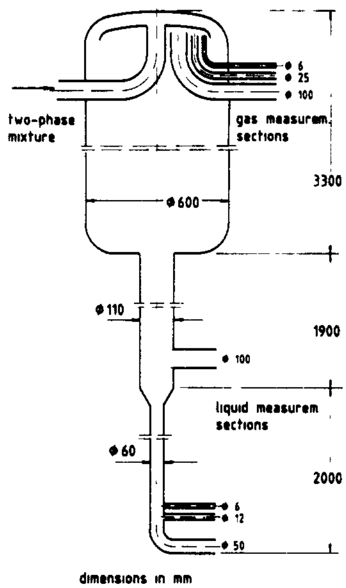

Figure 2. Gas–liquid separator.

which in some cases took several hours, the measurements started. The data were directly processed by a PDP 11/40 computer. These data included temperature, absolute and differential pressure readings in the inlet, branch and run measurement sections, and the differential pressure measurements in the test section. A computer program was set up which also took into account heat losses and flashing due to throttling of steam–water flow. The output values were mass fluxes and qualities for the inlet, branch and run related to the system pressure in the test section.

Figure 3 shows the matrix of the test points in flow pattern diagrams with the superficial velocities of the liquid and gas phases v_{sL1} and v_{sG1}, as the inlet parameters. Figure 3(a) contains the air–water test points; the parameter is the branch orientation. This test matrix includes flow patterns with fairly axisymmetric phase and velocity distributions, i.e. dispersed bubble flow. Furthermore, flow patterns were investigated with a distinct stratification due to gravity which correspond to test points near transition from slug to wavy flow and also test points located in the annular flow regime characterized by a bubbly mixture flowing at the bottom of the pipe and a thin liquid film at the top. Steam–water experiments were only performed with the horizontal branch. The parameter in figure 3(b) is the system pressure. The flow patterns belong to the slug or annular flow regime; the boundary between the flow regimes shifts to lower superficial gas velocities with increasing pressure (Reimann *et al.* 1981).

3. PHASE SEPARATION

3.1 Upward branch

In order to illustrate the phase separation in the next figures the quality ratio x_3/x_1 is plotted versus the mass flux ratio G_3/G_1. A value of $x_3/x_1 = 1$ corresponds to an equal phase split, i.e. no phase separation. The curve given by the relation

$$x_3/x_1 = (G_3/G_1)^{-1} \qquad [1]$$

is obtained if the total inlet gas flow enters the branch, which means the T-junction acts as a perfect separator. Figure 4 shows that a distinct phase separation occurs; the experimental results are very close to the total separation curve. The deviations from this curve are greatest for inlet flow patterns corresponding to the dispersed bubble flow regime. The influence of the inlet parameters is relatively small; therefore, this branch orientation was

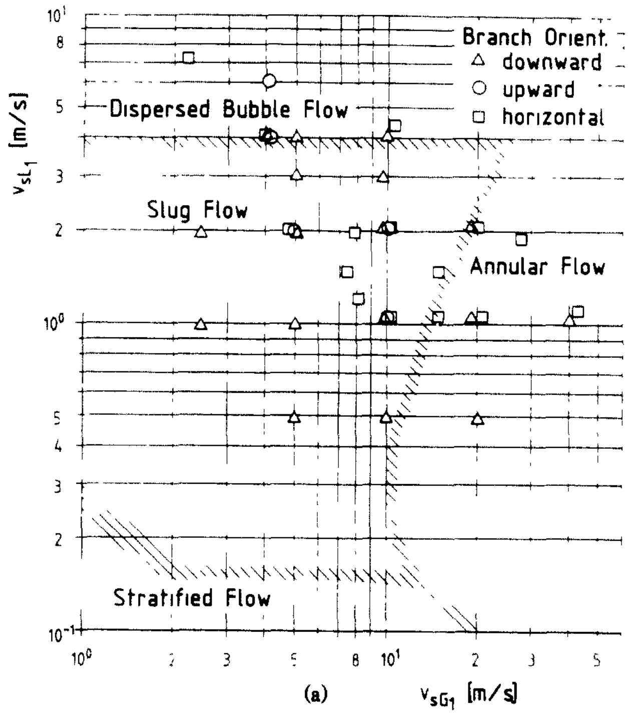

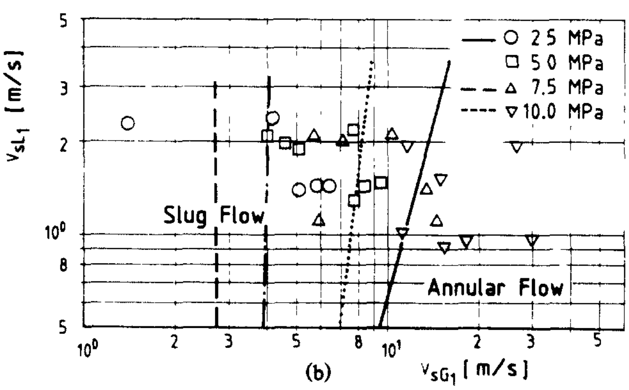

Figure 3. Inlet flow pattern diagram and test matrix. (a) horizontal air–water flow (p = 0.7 MPa); (b) horizontal steam–water flow.

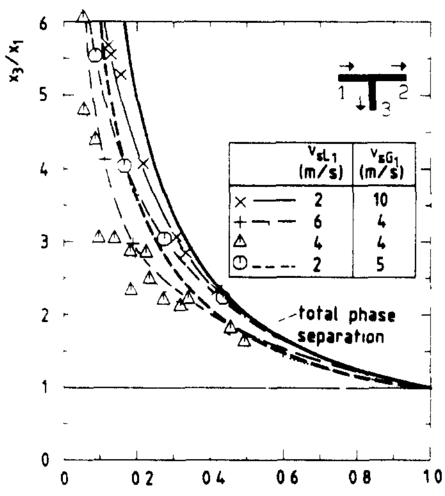

Figure 4 Phase separation for upward branch (air–water flow, p_1 = 0 7 MPa)

not investigated further in detail. For engineering design purposes, the following relationship is recommended:

$$x_3/x_1 = (G_3/G_1)^{-0.8} \quad . \qquad [2]$$

This relationship is plotted as a dashed curve in figure 4.

Equation [2] is not valid for very low values of G_3/G_1. In this range the branch quality x_3 is equal to 1, since liquid carryover does not occur. To estimate the maximum value of G_3 with $x_3 = 1$, the following relationship is recommended:

$$G_{3\max, x=1} = A \cdot 0.23\,(gD(\rho_L - \rho_G)\rho_G)^{0.5} \qquad [3]$$

with $A = 0.5$ for inlet conditions in the dispersed bubble flow regime and $A = 1$ for other inlet flow patterns. Relationships similar to [3] were used by Wallis (1969) to predict the transition between different flow regimes in vertical upward flow.

3.2 Horizontal branch

Figures 5 and 6 show typical results for the horizontal branch. All curves are quite close to the total separation curve for high values of G_3/G_1. They have a maximum in the vicinity of $G_3/G_1 = 0.3$ and then decrease quite rapidly with decreasing G_3/G_1. The extrapolated quality ratio for $G_3/G_1 = 0$ is $x_3/x_1 = 0$. This value is somewhat speculative, but seems to be reasonable, at least for flow patterns with liquid at the pipe wall, e.g. annular flow (compare, e.g. Azzopardi & Whalley 1982).

Figure 5 contains results for air–water flow at a system pressure of 0.7 MPa, a constant value of the superficial liquid velocity $v_{sL1} = 1$ m/s, and different values of the superficial gas velocity v_{sG1}. The phase separation decreases with increasing superficial gas velocity, which corresponds to an increasing gas momentum flux $(\rho v^2)_{G1}$.

In figure 6, results of steam–water and air–water flows are plotted for comparison. This figure shows the influence of the system pressure and phase densities, respectively, for test points with about the same values of the superficial velocities. The phase separation decreases with increasing pressure which again corresponds to an increasing gas momentum flux.

Following the idea of Azzopardi & Whalley (1982) who used the ratio of the local momentum fluxes of the phases to describe the phase separation for low values of G_3/G_1, the maximum of the curves $(x_3/x_1)_{\max}$ were plotted versus the ratio of the cross sectional phase momentum fluxes $(\rho v^2)_{G1}/(\rho v^2)_{L1}$. Introducing the velocity ratio in the inlet pipe $S_1 = v_{G1}/v_{L1}$, we obtain

$$(\rho v^2)_{G1}/(\rho v^2)_{L1} = (\rho_G/\rho_L)S_1^{\,2} \qquad [4]$$

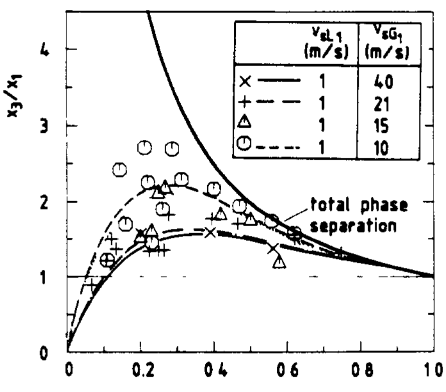

Figure 5. Phase separation for horizontal branch (air–water $p_1 \approx 0.7$ MPa; $v_{sL1} =$ const.).

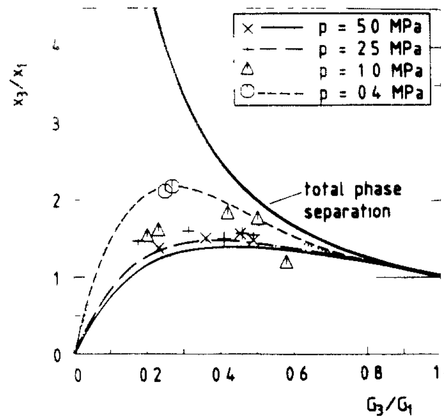

Figure 6. Phase separation for horizontal branch (air–water and steam–water flow, $v_{sL1} = 2$ m/s, $v_{sG1} = 10$ m/s).

In order to determine the velocity ratio in the inlet pipe, the correlation developed by Rouhani (1969) was used, given by

$$S_1 = \rho_L \frac{1}{1 - x_1}\left(\frac{1 + 0.12(1 - x_1)}{\rho_{h1}} + \frac{W_{rel}}{G_1} - \frac{x_1}{\rho_G}\right) \qquad [5]$$

where

$$\rho_{h1} = (x_1/\rho_G + (1 - x_1)/\rho_L)^{-1} \ ,$$
$$W_{rel} = (1.18/\rho_L^{0.5})/(g\sigma(\rho_L - \rho_G))^{0.25} \qquad [6]$$

and g is the acceleration due to gravity and σ the surface tension.

Figure 7 shows a semilogarithmic plot with the system pressure and the ratio of the superficial inlet velocities as parameters. Most of the test points are located quite close to the curve

$$(x_3/x_1)_{max} = ((\rho_G/\rho_L)S_1^2)^{-0.26} \qquad [7]$$

except for the test points located in the dispersed bubble flow regime. The implicit assumption

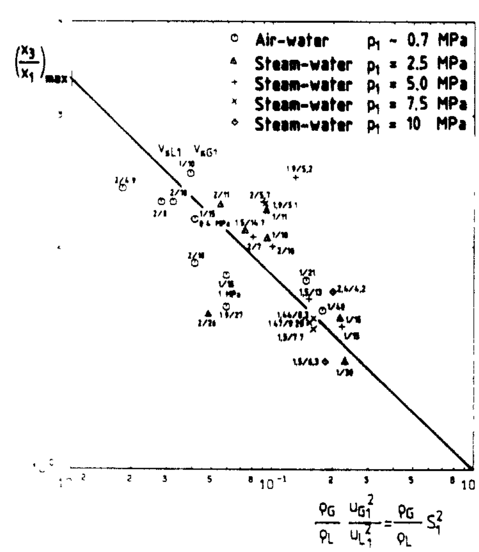

Figure 7 Dependence of phase separation maximum.

in the concept of the momentum fluxes resulting in [7] is that both phases can flow independently into the branch. This assumption is not valid for the dispersed bubble flow regime.

As a fitting curve for the phase separation, the following relationship is proposed.

$$x_3/x_1 = 5\eta - 6\eta^2 + 2\eta^3 + a \cdot \eta(1 - \eta)^b \qquad [8]$$

with $\eta = G_3/G_1$, and $b = 4$; $a = 14.6$ for test points in the dispersed bubble flow regime and

$$a = 13.9\left(\left(\frac{\rho_G}{\rho_L}S_1{}^2\right)^{-0.26} - 1\right) \qquad [9]$$

for other flow patterns. Equation [8] does not go to the correct limit $x_3 = x_1$ as the system pressure p approaches the critical pressure p_{crit}. Therefore, [8] should not be used at very high system pressures. The curves in figures 5 and 6 were calculated using [8] and [9].

Figure 8 shows the relative error between the measured and the predicted quality ratios x_3/x_1 as a function of the mass flux ratio G_3/G_1. The scatter is fairly symmetric around unity but can be quite large at low values of G_3/G_1. Here, measurement errors exert a great influence due to the steep gradient of the phase separation curve.

3.3 Downward branch

Figures 9 and 10 contain results for air–water flow and a constant value of v_{sL1} and v_{sG1}, respectively. For high values of G_3/G_1 the values x_3/x_1 are in general greater than 1, which means that the inertia effect is more pronounced than the gravity effect. At low values of G_3/G_1, x_3/x_1 is lower than 1, because the flow pattern in the inlet is dominating. Starting from $G_3/G_1 = 0$, there is a range where only liquid enters the branch ($x_3 = 0$). This range increases the more stratified the flow pattern is.

For constant value of v_{sL1} (figure 9), x_3/x_1 increases in general with increasing v_{sG1}; however, the effect is not very distinct. For v_{sG1} = const. (figure 10), x_3/x_1 increases considerably with increasing v_{sL1}. This is due to the fact that for varying v_{sG1} the flow patterns change more significantly than for varying v_{sL1}. This change is from a stratified type at low values of v_{sL1} to a more homogeneous type at $v_{sL1} = 4$ m/s. With increasing momentum fluxes, the curves tend to approach that curve where gravity is of no more influence, i.e. dispersed bubble flow or annular flow at high velocities.

For fitting the experimental data a first empirical approach is presented. Again a relationship equivalent to [8] is used. The exponent b is expressed as a function of the liquid

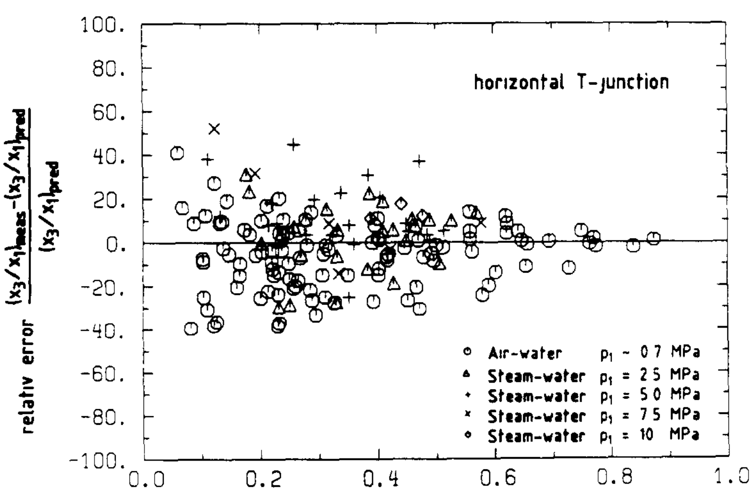

Figure 8. Relative error of predicted phase separation curves.

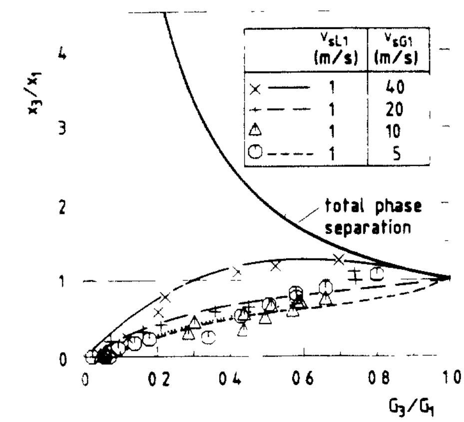

Figure 9 Phase separation for downward branch (air–water, p_1 = 0.7 MPa; v_{sL1} = const.)

mass flux:

$$b = 3 + 2.2 \tanh(0.5(G_1 - 3000)) \qquad [10]$$

whereas the factor a is dependent on both the liquid and gas mass flux as shown in figure 11.

In order to determine the maximum mass flux G_3 where x_3 is still zero, the following relationship is proposed:

$$G_{3\,\mathrm{max},x=0} = 0.52\, \rho_L^{0.5}(\sigma g(\rho_L - \rho_G))^{0.25} \qquad [11]$$

This is similar to the relationship for the rise velocity of bubbles given by Wallis (1969).

The final correlation for the phase distribution for the downward branch is then given by

$$x_3/x_1 = 5\eta - 6\eta^2 + 2\eta^3 + a\eta(1 - \eta)^b \qquad [12]$$

where

$$\eta = (G_3/G_1 - G_{3\mathrm{max},x=0} G_1)/(1 - G_{3\mathrm{max},x=0}/G_1) \quad . \qquad [13]$$

Again [12] is not valid at high pressures ($p \to p_{\mathrm{CRIT}}$). The exponent b is given by [10] and a is taken from figure 11. The curves plotted in figures 9 and 10 were calculated in this way.

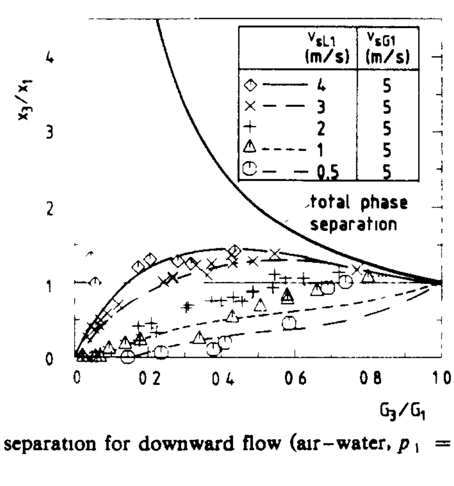

Figure 10. Phase separation for downward flow (air–water, p_1 = 0.7 MPa, v_{sG1} = const)

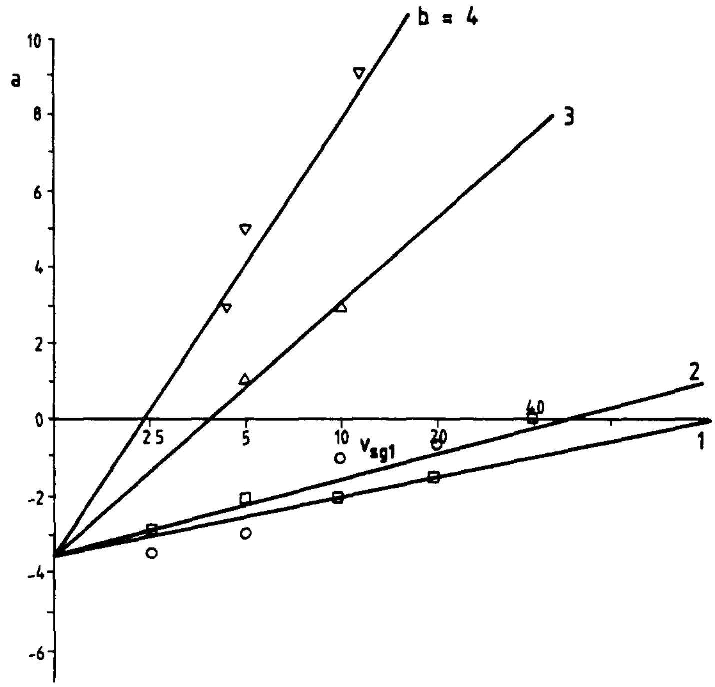

Figure 11. Dependence of factor a on liquid and gas mass flux.

4. COMPARISON WITH OTHER WORK

Investigations which are closely related to the present ones were performed by Saba & Lahey (1982), who used a horizontal T-junction, $d_3/d_1 = 1$, and inlet flow conditions (air–water flow) also covered by the present experiments. An inadequacy of their experiments was that they varied the mass flux ratio G_3/G_1 only in three steps: 0.3,0.5 and 0.7.

Figure 12 shows a comparison for air–water flow and superficial velocities of v_{sL1} = 2 m/s and v_{sG1} = 5 m/s. The results agree well for G_3/G_1 = 0.7 and 0.5. For G_3/G_1 = 0.3 the measured value from Saba & Lahey (1982) is higher; this is typical of all their results. Their data do not indicate a maximum in the curve since no data were taken for G_3/G_1 < 0.3.

Honan & Lahey (1981) used the same T-junction and inlet parameters as Saba & Lahey but performed experiments with a vertical upward inlet flow direction. The results were very close to those obtained with the horizontal T-junction.

A similar tendency is observed if the present results are compared with the results obtained by Zetzmann (1982), who also used a vertical upward inlet flow direction and a

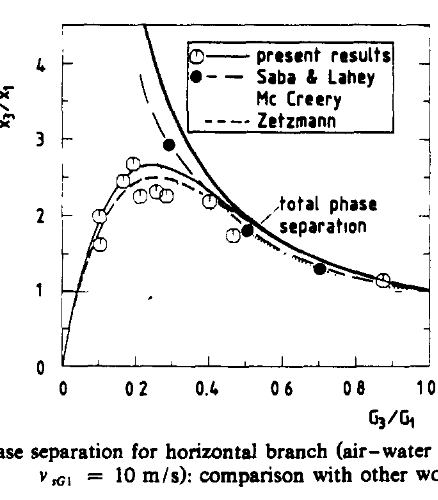

Figure 12. Phase separation for horizontal branch (air–water flow, v_{sL1} = 2 m/s, v_{sG1} = 10 m/s): comparison with other work.

horizontal branch. Figure 12 contains the fitting curve proposed by Zetzmann; the agreement is surprisingly good for the test point chosen. The relationship proposed by Zetzmann does not take into account the influence of any flow parameters such as G_1, x_1 and system pressure p_1; the validity should therefore be restricted to the parameter range investigated (air–water flow, bubbly and slug flow patterns).

Saba & Lahey (1984) developed a phase separation model based on their experiments which assumes constant values for the void fraction and the phase velocities in the cross section. Similar assumptions were used in a model by McCreery (1983) who used preliminary measurements from Reimann *et al.* (1980) to adjust his model. The corresponding curves are also shown in figure 12. The phase separation is predicted satisfactorily for the range $G_3/G_1 > 0.5$ where the values are close to the total separation curve, but the agreement is lacking in the lower parameter range.

A model, based on void fraction and phase velocity distributions in the cross section, together with local momentum fluxes was proposed by Azzopardi & Whalley (1982) and Azzopardi & Baker (1981). This model gives good results for low values of G_3/G_1 but again does not predict the maximum of the curve.

A combination of the two concepts was used by Lahey *et al.* (1985) to propose a general relationship for the total range of G_3/G_1. However, a physical model for the intermediate range of G_3/G_1 has not been incorporated yet; therefore, only the high and low ranges of G_3/G_1 are predicted satisfactorily.

Contributions related to the present work for a *T*-junction with horizontal inlet but vertical upward or downward oriented branches are even more limited. Therefore, no comparisons are possible.

5 CONCLUSIONS

Up to now it has not been possible to predict satisfactorily the phase separation for arbitrary flow conditions and geometries of *T*-junctions. All experimental and theoretical contributions to this subject cover only a limited range of parameters.

In the presented work, two-phase flow has been investigated in a *T*-junction with equal pipe diameters, horizontal inlet flow and different branch orientations:

—For vertical upward branch flow, a strong phase separation occurs, because inertia and gravity effects act in the same direction. An empirical relationship is given for the phase separation effect. For more detailed modeling, the flow behavior in the branch must also be taken into account.

—With the horizontal branch, extensive air–water and, for the first time, steam–water experiments were performed. Previously published models predict satisfactorily the phase separation in the lower and high ranges of G_3/G_1. Within the scope of the present investigations a simple phase separation model is presented which fills the gap between these other models. Further work is necessary to develop models based on more sophisticated physical concepts.

—For the downward branch, inertia and gravity act in different directions; the phase distribution in the inlet pipe has a strong influence on the phase separation in the branch. Up to now no adequate model is available to account for these influences.

REFERENCES

AZZOPARDI, B. J. & BAKER, S. R. 1981 Two phase flow in a "*T*"-junction: The effect of flow pattern in vertical upflow. AERE-R 10174, June.

AZZOPARDI, B. J. & WHALLEY, P. B. 1982 The effect of flow patterns on two-phase flow in a *T*-junction. *Int. J. Multiphase Flow* **8**, 491–507.

HENRY, J. A. R. 1981 Dividing annular flow in a horizontal tee. *Int. J. Multiphase Flow* **7**, 343–355.

HONAN, T. J. & LAHEY, R. T. 1981 The measurement of phase separation in wyes and tees. *Nuclear Engineering and Design* **64**, 93–102.

JOHN H. & REIMANN, J. 1979 Gemeinsamer Versuchsstand zum Testen und Kalibrieren verschiedener Zweiphasen-Massenstrommeßverfahren, Anlagenbeschreibung. KfK 2731 B.

LAHEY, R. T., AZZOPARDI, B. J. & COX, M. 1985 Modelling two-phase flow division at *T*-junctions. *2nd Int. Conf. on Multi-Phase Flow*, London, England, 19–21 June.

MCCREERY, G. E. 1984 A correlation for phase separation in a tee. *Multi-Phase Flow and Heat Transfer III. Part B: Applications* (Edited by Veziroglu, T. N. and Bergles, A. E.). Elsevier, Amsterdam.

REIMANN, J., SEEGER, W. & JOHN, H. 1980 Erste Experimente zur Umverteilung einer Luft-Wasser-Strömung in einem T-Stück. Kernforschungszentrum Karlsruhe, unpublished.

REIMANN, J., JOHN, H. & SEEGER, W. 1981 Transition from slug to annular flow in horizontal air–water and steam–water flow. KfK 3189.

ROUHANI, Z. 1969 Modified correlations for void and two-phase pressure drop. AE-RTV-8841.

SABA, N. & LAHEY, R. T. 1982 Phase separation phenomena in branching conduits. NUREG/CR-2590.

SABA, N. & LAHEY, R., JR. 1984 The analysis of phase separation phenomena in branching conduits. *Int. J. Multiphase Flow* **10**, 1–20.

SEEGER, W. 1985 Untersuchungen zum Druckabfall und zur Massenstromumverteilung von Zweiphasenströmungen in rechtwinkligen Rohrverzweigungen. Dissertation, Universität Karlsruhe, KfK 3876.

SEEGER, W., REIMANN, J. & MUELLER, U. 1985 Phase separation in a *T*-junction with a horizontal inlet. *2nd Int. Conf. on Multi-Phase Flow*, London, England, 19–21 June.

SMOGLIE, C. & REIMANN, J. 1986 Two-phase flow through small branches in horizontal pipe with stratified flow. *Int. J. Multiphase Flow* **12**, 609–625.

WALLIS, G. B. 1969 *One-Dimensional Two-Phase Flow*, McGraw-Hill, New York.

ZETZMANN, K. 1982 Phasenseparation und Druckabfall in zweiphasig durchströmten vertikalen Rohrabzweigungen. Doctorate Thesis, University of Hannover, FRG.